Vertical profiles of CO_2 above eastern Amazonia suggest a net carbon flux to the atmosphere and balanced biosphere between 2000 and 2009

By L. V. GATTI[1]*, J. B. MILLER[2,3], M. T. S. D'AMELIO[1], A. MARTINEWSKI[1], L. S. BASSO[1], M. E. GLOOR[4], S. WOFSY[5] and P. TANS[2], [1]*Instituto de Pesquisas Energéticas e Nucleares (IPEN), Atmospheric Chemistry Laboratory, São Paulo 05508-000, Brazil;* [2]*National Oceanic and Atmospheric Administration (NOAA), Earth System Research Laboratory, Boulder, USA;* [3]*Cooperative Institute for Research in Environmental Sciences (CIRES), University of Colorado, Boulder, USA;* [4]*University of Leeds, United Kingdom;* [5]*Harvard University, Cambridge, MA, USA*

ABSTRACT

From 2000 until January 2010 vertical profiles were collected above eastern Amazonia to help determine regional-scale ($\sim 10^5$–10^6 km^2) fluxes of carbon cycle-related greenhouse gases. Samples were collected aboard light aircraft between the surface and 4.3 km and a column integration technique was used to determine the CO_2 flux. Measured CO_2 profiles were differenced from the CO_2 background determined from measurements in the tropical Atlantic. The observed annual flux between the coast and measurement sites was 0.40 ± 0.27 gC m^{-2} d^{-1} (90% confidence interval using a bootstrap analysis). The wet season (January–June) mean flux was 0.44 ± 0.38 gC m^{-2} d^{-1} (positive fluxes defined as a source to the atmosphere) and the dry season mean flux was 0.35 ± 0.17 gC m^{-2} d^{-1} (July–December). The observed flux variability is high, principally in the wet season. The influence of biomass burning has been removed using co-measured CO, and revealed the presence of a significant dry season sink. The annual mean vegetation flux, after the biomass burning correction, was 0.02 ± 0.27 gC m^{-2} d^{-1}, and a clear sink was observed between August and November of -0.70 ± 0.21 gC m^{-2} d^{-1} where for all of the dry season it was -0.24 ± 0.17 gC m^{-2} d^{-1}.

1. Introduction

The Amazon basin covers one of the largest forested areas globally, about 8 million km^2, constitutes the largest reservoir of above-ground organic carbon and hosts one quarter of global biodiversity (Malhi and Phillips, 2005). It is under strong human pressure through logging, forest conversion and other forms of resource exploitation. Most importantly in the context of carbon balance, its response to a warming climate and uncertain changes in precipitation regime are the matter of intense debate (e.g. Cox et al., 2000; Friedlingstein et al., 2001; Friedlingstein et al., 2006; Lapola et al., 2009). Specifically, some models project large reductions in above-ground biomass including transitions in eastern Amazonia from forest to savannah. Regardless of the accuracy of the predictions, the size of the Amazonian carbon reservoir implies significant potential cou-

pling between the Amazonian carbon cycle, global climate and global greenhouse gas burdens of CO_2, CH_4 and N_2O.

Net carbon balance is a central diagnostic of the state and changes of the land surface, and its knowledge is a pre-requisite for evaluating the skill of predictive coupled carbon-climate models. However, whether the Amazon is even a net source or sink of carbon remains unknown. Estimates exist of fluxes associated with contributing processes such as deforestation (Defries et al., 2002; Houghton, 2003; Van Der Werf et al., 2004), along with evidence for responses of undisturbed rainforests to a changing environment (Phillips et al., 1998), but their values vary widely. Additionally, eddy covariance and biometry studies representing spatial scales of 1 hectare to 1 km^2 have shown widely disparate net flux results, from the large sink first reported by Malhi et al. (1998) from a site in central Amazonia, to the moderate net source for a site in eastern Amazonia shown by Saleska et al. (2003) [see review by Ometto et al. (2005)]. In addition to these small spatial scale studies, a few regionally representative short-term studies of Amazonian carbon balance using aircraft (Wofsy et al., 1988; Chou et al., 2002; Lloyd et al.,

2007) have not suggested either large sources or sinks of carbon over their study periods. Global atmospheric inversions of CO_2 measurements at remote sites have also resulted in widely disparate estimates of tropical South American carbon balance ranging from sinks of up to 0.9 ± 1.1 PgC yr^{-1} (Gurney et al., 2002) to a source of 3.1 ± 2.4 PgC yr^{-1} (Jacobson et al., 2007). It should be noted that these inverse model estimates are associated with large formally calculated uncertainties that stem from the absence of CO_2 mole fraction time series at locations with significant influence from the Amazonian land surface. Thus, in these inversions, Amazonia is essentially unconstrained, and its fluxes are determined as a residual of the global mass balance. However, a recent re-analysis of the Transcom CO_2 inversion intercomparison models by Stephens et al. (2007) suggested that uncertainties in modelled vertical transport could explain most of the tropical flux variability across models. When Northern Hemisphere airborne CO_2 data were used as a consistency check, the models satisfying this check were close to neutral (including deforestation) across the tropics. Even after discounting some of the largest estimates like those of Malhi et al. (1998) due to known issues with nighttime eddy covariance artifacts (e.g. Goulden et al., 1996) and the range encompassed by the Transcom inversions, the overall the basin could be a net source of more than 1 PgC yr^{-1}, or a net sink greater than 1 PgC yr^{-1}. This 2 PgC yr^{-1} range is equivalent to more than 20% of global fossil fuel emissions in the year 2008.

Fundamentally, carbon observations in Amazonia have suffered from a serious 'scale-gap', which has directly led to these large uncertainties. That is, most of the carbon balance studies to date have focused on either very small spatial scales (biometry and eddy covariance), which require a large degree of extrapo-lation, or global scale inversions, which fail to constrain tropical land masses even at the continental scale. Some of the aforementioned airborne campaigns have given a regional flux picture, but over a period too small to determine annual net fluxes. In this paper, we present an alternative way to examine net carbon fluxes in Amazonia, by making regular vertical profiles of CO_2 and other greenhouse gases (Miller et al., 2007; D'Amelio et al., 2009) that are representative of regional scales ($\sim 10^5$–10^6 km^2). Although the single vertical profile site presented here is sensitive only to a fraction of the basin, it suggests a way forward to derive robust, integrated and basin-wide fluxes.

An integral diagnostic of the Amazon carbon balance is provided by the accumulation or depletion of CO_2 of the atmospheric air volume above the Amazon. An estimate of the accumulation and depletion of CO_2 in air travelling over the continent can be obtained using regular vertical aircraft-based CO_2 profile measurements. Here we report on results of such measurements performed near Santarem, in the state of Pará in eastern Amazonia since December 2000. Specifically we have measured CO_2, CH_4, N_2O, CO, H_2 and SF_6. In combination with the background records of these gases at Barbados and Ascension Island measured by NOAA/ESRL we estimate monthly mean carbon flux characterizing about 20% of the Brazilian Amazon ($\sim 5 \times 10^6$ km^2). This technique is made possible by the consistent easterly trade winds that extend from the surface to the top of our aircraft profiles (~ 4 km asl), which implies that our vertical profile measurements are sensitive to the integrated flux from the region extending from the Atlantic coast to Santarem (Fig. 1). Using CO measurements in our flasks, we also estimate the contribution to our signals from biomass burning to obtain CO_2 fluxes from the land vegetation alone. We will first
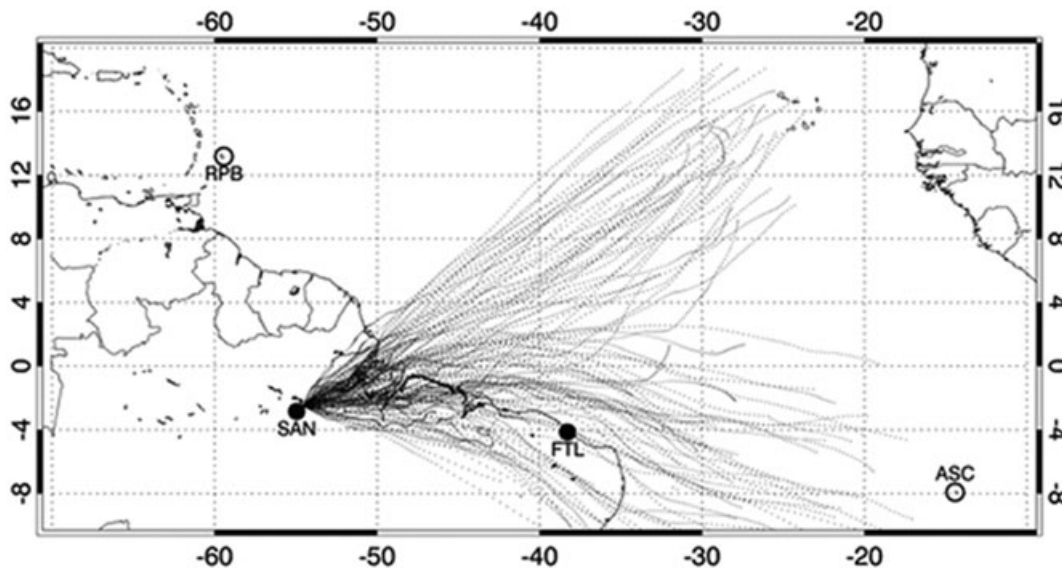

Fig. 1. NOAA/ESRL (open circles) and IPEN sampling sites (closed circles) used in this study. Dots show hourly positions of 5-d backtrajectories arriving at SAN at 1500, 1000 and 500 m asl for all vertical profiles sampled between December 2000 and December 2007. Dots are plotted only when the altitude of the backtrajectory is less than 1500 m asl.

introduce the site, measurement method and schedule. We will then explain and apply the CO_2 flux estimation method and finally discuss the results and its implications for the net Amazon carbon balance.

2. Methods

2.1. Site, region of influence and sampling procedure

The aircraft vertical profile measurements that we report here started in December 2000 with flights above the Tapajós National Forest in the state of Pará, Brazil ($2°51.42'$S, $54°57.54'$W), near the city of Santarém (Fig. 1). Between December 2000 and January 2010 we measured 98 profiles of CO_2, CH_4, CO, N_2O, SF_6 and H_2, with a small subset also having been analysed for $\delta^{13}C$ of CO_2. This site will be referred to in this paper as SAN. Air was collected with portable sampling systems consisting of separate compressor and flask units (Tans et al., 1996). These units are loaded onto a light aircraft (Cessna 206) and draw ambient air via a sampling tube (Bevaline—3/8″ o.d., 1/4″ i.d.) sticking out from the right-wing vent approximately 1m from the cabin. Since 2007, a GPS and temperature and relative humidity sensors have also been attached to the compressor unit. The pilot initiates sample collection at a pre-determined altitude using a wired remote control. The flask unit contains 17 flasks each with 700 mL and pressurized to about 270 kPa. Between 2000 and 2006, flights consisted of one descending and one ascending profile from 3600 m to 300 m. Since that time, samples were collected during one descending spiral profile from 4300 m to 300 m asl. From 4300 m down to 1200 m we sampled every 300 m and from 1200 m onwards every 150 m down nearly to the canopy height. Profiles were usually taken between 12–14 hours local time, because this is the time when the boundary layer is close to being fully developed. It also represents the time at which the column average is most similar to the daily mean (Chou et al., 2002).

Between 2000 and 2003, samples were sent for analysis to the NOAA/ESRL laboratory in Boulder, USA. Measurement precision for CO_2 at the NOAA laboratory is estimated to be better than 0.05 ppm. Since 2004, we have started to operate a replica of the NOAA analysis system in Brazil at Instituto de Pesquisas Energeticas e Nucleares (IPEN), with precision and accuracy very similar to that at NOAA (0.04 ppm). Besides the aircraft data from SAN, the analysis presented in this paper also uses data from Ascension Island (ASC—7.92 S, 14.42 W) and Barbados (RPB—13.17 N, 59.43 W), which are part of the NOAA Earth System Research Laboratory (NOAA/ESRL) global air-sampling network. At these ground-based stations air was sampled with 2.2 L glass flasks with Teflon-tipped glass stopcocks. The flasks were filled to about 120 kPa (Conway et al., 1994), and shipped to NOAA/ERSL for analysis of the same suite of gases. All SAN measurements presented here are available via an anonymous ftp at ftp.cmdl.noaa.gov/pub/LBA;

RPB and ASC measurements are available at ftp.cmdl.noaa.gov/ccg/co2.

At SAN, profiles were made above the Tapajos National Forest, near the km 67 eddy covariance tower (Saleska et al., 2003) which is located around 20 km to the east of the Tapajos river. From December 2000 until 2005, on 33 sampling days, profiles were taken in parallel. The first location was above the tower and the other was approximately 30 km to the east of the tower. This was done to determine (1) the impacts of fluxes from the river (e.g. Richey et al., 2002), although CO_2 fluxes from this part of the Tapajos river are likely to be very small (J. Richey, personal communication, 2005) and (2) the degree to which local fluxes could influence the CO_2 profiles. The second measurement location is above a pasture landscape. In order to sample the vertical structure of background air for the Amazon basin, between 2000 and 2003, 11 vertical profiles were collected 50 km northeast of Fortaleza, Ceará state (Fig. 1; site code FTL $4°09'$S, $38°16'$W), over the Atlantic ocean.

The region upwind of SAN to which our measurements are sensitive is characterized by moist tropical forest in the immediate vicinity as well as to the east along the Amazon and to the northeast. In the southeast sector, there has been a considerable amount of forest clearing in eastern and southern Para, which is still ongoing as evidenced by the CO signals we observe. Further to the southeast, backtrajectories indications suggest some additional influence from *cerrado* (wooded savannah) and scrubland of the northeastern states of Maranhão, Piaui and Ceará. Overall, based on existing vegetation maps and backtrajectories, we expect our signal to be dominated by the influence of intact and degraded moist tropical forest landscapes.

2.2. CO₂ measurement

There are two primary challenges in CO_2 measurement: precision or more formally 'repeatability' and accuracy or more formally 'measurement trueness' (VIM3, 2007). In our case, precision is needed to have the sensitivity to identify small changes in concentration within a given vertical profile. But accuracy is by far the most important here, because we are combining measurements from two independent laboratories in this study and need to be sure that observed SAN minus background differences are geophysical and not an artifact of calibration differences between IPEN and NOAA. Furthermore we need to ensure that any trends observed in the data are not artifacts of the sample analysis switching from the NOAA to IPEN labs in 2004. In order to achieve this, measurements at both IPEN and NOAA are both tightly linked to the WMO CO_2 mole fraction scale.

CO_2 is measured using an NDIR analyser (Licor Li-7000) which is operated in a configuration with a reference gas of about 330 ppm in the reference cell and reference gases ranging from about 360 to 400 ppm as well as sample gas in the sample cell. Despite the factory linearization of the Li-7000, a three-point calibration is used, with NOAA calibrated reference gas alternating
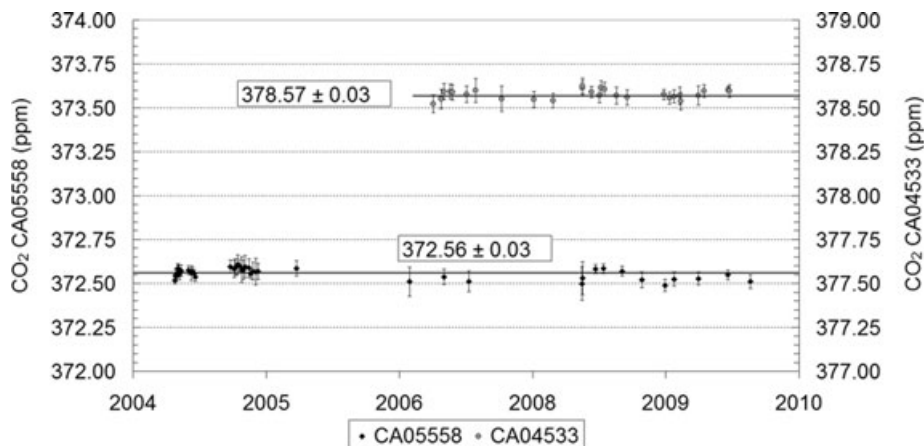
Fig. 2. Time series for the tanks CA05558 (diamonds) and CA04533 (circles). Each small point represents the mean of 20 aliquots by tank calibration; the error bars represent the standard deviation of the 20 analyses. The repeatability is the standard deviation of the results of all tank calibrations (2004–2009). The stability of tank CA05558, especially, demonstrates the long-term repeatability of our system. The Tank CA04533 calibrated by NOAA show a 378.60 ± 0.03 ppm, compared with 378.57 ± 0.03 ppm obtained at IPEN give us the accuracy inside the standard deviation of measured concentration at NOAA.

with sample aliquots in the following sequence: Ref-hi, sample, Ref-mid, sample, Ref-low, sample, Ref-mid, sample, Ref-hi, etc. Thus, for every two samples, one calibration curve is calculated. This mode of operation is also employed at NOAA/ESRL. In order to assess both the accuracy and long-term repeatability of the CO_2 measurements, a previously calibrated tank is measured as an unknown on the system on a regular basis. The results of these 'target' tanks show long-term repeatability of 0.03 ppm and a difference between measured and calibrated values of 0.03 ppm (Fig. 2). The calibrated mole fraction at NOAA was 378.60 ± 0.03 ppm and at IPEN tank calibration was 378.57 ± 0.03 ppm, showing a high level of agreement between them. Additionally, an intercomparison in operation since October 2006 of flasks sampled by IPEN and NOAA, taken within 30 min of each other at the Arembepe site on the Atlantic coast (12.5S, 38.1W) and analysed by NOAA and IPEN show a mean difference of only +0.02 ppm (IPEN minus NOAA).

2.3. CO_2 flux calculation

In order to study the CO_2 accumulation or depletion along the path of air volumes travelling from the coast over land until the profile site, we use an air column integration technique which does not need to account for exchange between the convective boundary layer (CBL) and free troposphere, first described by Chou et al. (2002). Miller et al. (2007) used this technique and added the use of the difference between the observed column and the marine background. This technique needs an estimate of the background CO_2 mixing ratio, which is the concentration in the air mass that enters the continent at the Atlantic coast within the latitude band between approximately 2°N to 10°S latitude of the Amazon, Brazil. From Fig. 1 it is apparent that equa-

torial sites like SAN sample both Northern (NH) and Southern Hemisphere (SH) air, depending on the location of the Inter-Tropical Convergence Zone (ITCZ). Thus it is necessary for the application of the air column integration technique to select background concentration values dynamically as described below.

2.3.1. Background calculation. In order to estimate the relative NH and SH contributions to the background value, we use the median values of sulphur hexafluoride (SF_6) from SAN vertical profiles and interpolated values from the ASC and RPB time series. The measurement precision of SF_6 is about 0.4% (0.02 ppt), which is similar to the typical variability in the SAN SF_6 vertical profiles. SF_6 is mainly used as an insulator in electrical switching stations and thus is strongly tied to energy consumption (e.g. Maiss et al., 1996; Gloor et al., 2007). Because energy consumption is much larger in the Northern Hemisphere compared to the Southern Hemisphere, high values of SF_6 indicate Northern Hemisphere air and vice versa. There are essentially no emissions of SF_6 between the coast and our sites (Olivier et al., 1999) so that all variations seen at our aircraft sites result from varying amounts of NH and SH tropical air. Most of the time SF_6 mole fractions are bounded by ASC and RPB (Fig. 3a). They sometimes exceed these bounds, though, suggesting an effective air origin further north or south, respectively, of RPB or ASC.

Using a simple two-end-member mixing model (Miller et al., 2007), we calculate the fractions of air arriving at our Amazonian site due to NH (RPB) and SH (ASC) air

$$f_{ASC} = \frac{SF_{6-SAN} - SF_{6-RPB}}{SF_{6-ASC} - SF_{6-RPB}} = 1 - f_{RPB}. \tag{1}$$

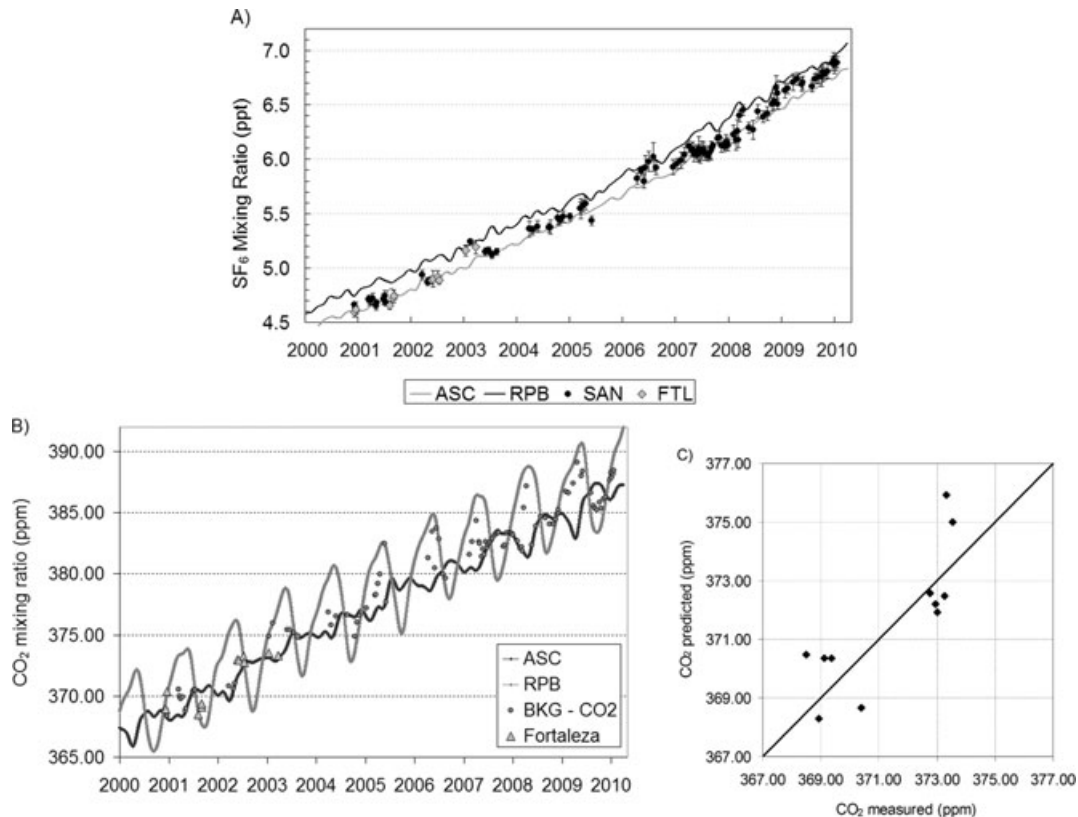$$X_{bg} = f_{ASC} X_{ASC} + (1 - f_{ASC}) X_{RPB}. \tag{2}$$

Fig. 3. (a) SF_6 time series from Ascension Island ASC (grey line), Barbados Island RBP (black line), SAN average vertical profile (black circle) and Fortaleza average vertical profile (grey lozenge). (b) CO_2 time series from Ascension Island ASC (grey line), Barbados Island RBP (black line) and CO_2 BKG calculated by eq. 2 (black circle) and Fortaleza average vertical profile (grey diamond). (c) Correlation between CO_2 background predicted by SF_6 method and CO_2 measured in Fortaleza profile, where the correlation coefficient (r^2) is 0.7.

f_{ASC} is the fraction of air arriving at SAN originating from the latitude of ASC, SF_{6-SAN} is the median SF_6 value from the SAN vertical profile. $SF_{6(ASC\,or\,RPB)}$ is the SF_6 mole fraction extracted from a smoothed curve fit (Thoning et al., 1989) to the SF_6 record of ASC or RPB from the 3 d before a given SAN vertical profile. *X* refers to the mole fraction of any gas co-measured with SF_6, in this case, CO_2. We allow f_{ASC} and f_{RPB} to exceed 0 and 1, but bound them at −0.5 and +1.5. This algorithm, including the extension of values below 0 and above 1 assumes that SF_6 and CO_2 meridional gradients in the tropical Atlantic are both linear between about 18°S and 23°N (although values of f_{RPB} rarely exceed 0.5, meaning that the northern linearity criterion need only be met to 13°N, the latitude of RPB). This linearity requirement is generally accurate, but deviations from it contribute to uncertainty in our flux calculation. The bounds we place on f_{ASC} and f_{RPB} reflect caution in assuming linearity much further to the north or south of our background sites; when f_{ASC} and f_{RPB} exceed the bounds, we use values of 0 (<0) and 1.0 value (>1.5).

As a consistency test the CO_2 background values obtained by this method are compared in Fig. 3b with the smoothed ASC and RBP CO_2 records. As expected the estimated background

values are mostly between the ASC and RPB concentrations. For fractions higher than 1.00 (lower than ASC) the concentration is a little smaller than ASC. This is because some of the air comes from further south than ASC (confirmed by air mass trajectories).

We tested our background model calculation using 11 vertical profiles measured at FTL (Fig. 3c). We used the SF_6 from these profiles to calculate the fractions (eqs 1 and 2) and applied this to CO_2 measured at ASC and RBP. We thus obtained predicted CO_2 background values and compared them with CO_2 measured in the FTL profiles. We found a correlation (r^2) of 0.7 (Fig. 3c), showing consistency between X_{bkg} predicted by SF_6 method and the column integral of CO_2 at the coast near FTL.

2.3.2. CO_2 flux estimation. Air entering the Amazon basin accumulates flux from the surface along its path to SAN. Thus, the difference between our SAN measurements and the Atlantic background should be directly related to terrestrial CO_2 fluxes from all source and sink processes, known and unknown, including NEE of native and agricultural ecosystems, river evasion (Richey et al., 2002), agricultural land cover change including combustion and any fossil fuel combustion. The differenced profiles (SAN minus background) can be converted to surface fluxes
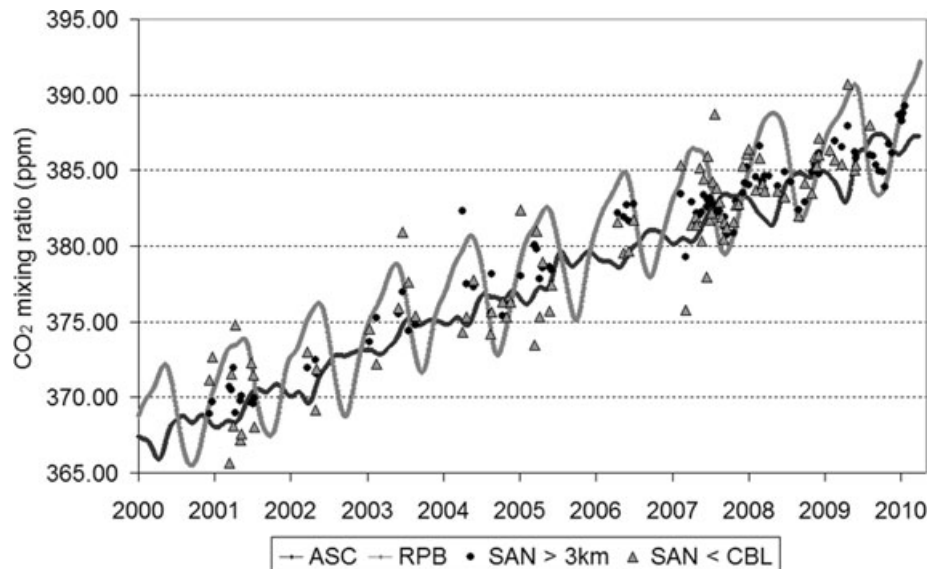
Fig. 4. CO_2 time series, marine boundary layer sites Ascension Island (grey line), Barbados (black line) and SAN vertical profile average above of 3 km and below 1200 m ($\sim$CBL).

by integrating the CO_2 from the surface to the top of the profile, and dividing by the travel time (t) of the air parcel from the coast to the place where the profile was measured (SAN) (Miller et al., 2007).

$$F_{CO_2} = \frac{\int_{z=0}^{4\,km} \left([CO_2]_{site} - [CO_2]_{bg}\right)\,dz}{t}. \qquad (3)$$

$[CO_2]$ is the concentration of CO_2 in μmol m^{-3}, which was determined from SAN CO_2 observations and vertical profiles of temperature and pressure calculated assuming a constant lapse rate of 6.5 K km^{-1} and a scale height of 7 km. The travel time t is calculated by backtrajectories simulated by the HYSPLIT model (Fig. 4). Trajectories were calculated in 500 m steps starting from 500 m up to 4000 m (Draxler and Rolph, 2003). Note that when a backtrajectory reached a level lower than 50 m a.g.l. over the continent, a default value of 2 d was used for t. Our approach is the same as that of D'Amelio et al. (2009) and a slight improvement over the approach of Miller et al. (2007), who used a constant value for t of 2 $\pm$ 1 d. Sensitivity tests, for N$_2$O (D'Amelio et al., 2009), showed that using a nominal value of 2 d did not significantly affect annual or seasonal flux averages.

Backtrajectories simulated by the HYSPLIT model confirm the earlier statement based on SF$_6$ observations that air arriving at SAN comes from both hemispheres. The land area encompassed by the backtrajectories observed in Fig. 1 is the representative area for our flux results. This area, when all profiling days are considered, covers between 0.5 and 1 million km^2. Lagrangian particle dispersion modelling results (not shown) suggest the area significantly influencing any single profile is closer to 100 000 km^2.

3. Results and discussion

3.1. Observed vertical gradients

One basic way to understand the terrestrial trace gas sources and sinks is to compare the observed mole fractions at site with background mole fractions either from the free troposphere at the same latitude and longitude (e.g. Lloyd et al., 2007) or a remote background site (e.g. Miller et al., 2007). Site mole fractions higher than background indicate sources along the back-trajectory and those lower indicate sinks, because the air column picks up flux contributions along its path. For the 98 profiles we analyse here (Fig. 4) the annual mean difference between the free troposphere and the CBL at SAN is -0.07 ± 1.20 ppm, suggesting a near neutral upwind surface carbon flux. As rough estimates, we define the free troposphere as the air column above 3 km asl and the CBL as below 1.2 km asl, based on typically observed CO_2 vertical profiles (Fig. 5). Vertical gradients in the wet season (January to June) average 0.51 ± 1.31 ppm, suggesting a net source in wet season and those in the dry season (July to December) average -0.64 ± 0.81 ppm, suggesting a net sink in the dry season.

3.2. Surface CO_2 fluxes

Although vertical gradients have previously been employed to estimate surface carbon fluxes (e.g. Lloyd et al., 2007), our approach here is to estimate the net carbon flux for eastern Amazonia by using the column integration technique described earlier. This method avoids the issue of convective redistribution of fluxes above the CBL top, which boundary layer budgeting techniques cannot deal with. As can be seen from eq. 3, we do
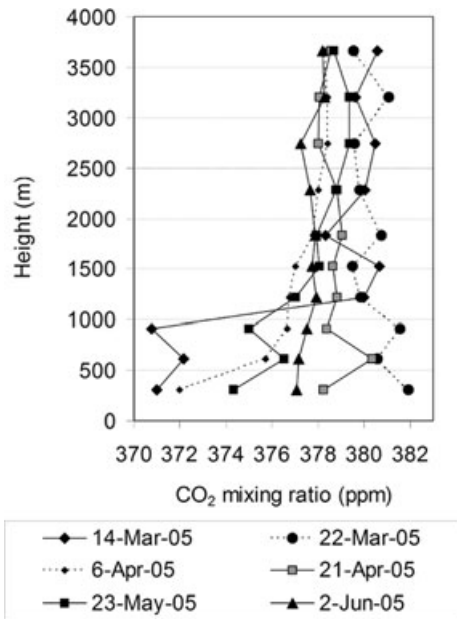
Fig. 5. Vertical profiles at SAN during wet season of 2005.

not need to assume anything about the maximum CBL height or anything about exchange terms (entrainment and/or detrainment) across the top of the CBL. Furthermore, in Amazonia, where convective processes are extremely important components of mass transport, even over the ~2 d time scales we are investigating, assuming a static-free troposphere reservoir could result in significant biases. Also, as can be seen in Fig. 5, some profiles do not have well-defined CBL, free troposphere transitions. Theoretically, the column integration technique is an ideal method if one can fly above the height reached by convection. Convection (both dry and moist) transports air masses from the CBL boundary aloft allowing carbon to be lost or gained from higher altitudes. In our study, the vertical profiles were made up to a maximum of 4.3 km asl. Thus, convective re-distribution of

fluxes (positive or negative) above this altitude will be neglected in our approach (see 3.4.2 for quantitative error analysis).

Individual and monthly mean flux results calculated using eq. 3 is shown in Fig. 6. During the early wet season (January and February) monthly mean fluxes are positive, especially so in February.

In January there is also a positive flux, but for 2 of 7 profiles the rainy season had not yet started upwind of SAN. For these two profiles co-measured CO and CH$_4$ clearly reveal that the signal comes from biomass burning. From March to October, the mean flux is zero, although it is clear from looking at the individual flux results that the flux variability is high (principally during February and March) and source and sink instances are being balanced. Fluxes exhibit lower variability between April and November. Finally, during November and December, there is a flux to the atmosphere. Since seasonal precipitation is clearly a major control on fluxes, we have calculated precipitation averages for four box-shaped regions [(a) Latitude from 2° to −4° and longitude from −55° to −32°; (b) Latitude from −4° to −6° and longitude from −50° to −32°; (c) Latitude from −6° to −8° and longitude from −45° to −32° and (d) Latitude from −8° to −10° and longitude from −40° to −32°] in the region upwind of SAN (Fig. 7) from gridded satellite-based precipitation estimates (http://hydis8.eng.uci.edu/hydis-unesco/, Hydrologic Data and Information System). For these four regions, on average the rainy season starts in January and ends in June. Unlike small-scale biometry and eddy-covariance measurements, our regionally representative measurements are sensitive not only to NEE but also biomass burning in the region, which tends in this area to start in August (Fig. 8). Biomass burning is most intense in October and November and usually stops in December. Therefore we define here the periods from January to June as wet season and calculate a mean flux of 0.44 ± 0.38 gC m^{-2} d^{-1} and the dry season from July to December to obtain a mean flux of 0.35 ± 0.17 gC m^{-2} d^{-1}. The annual flux mean is 0.40 ± 0.27 gC m^{-2} d^{-1}.
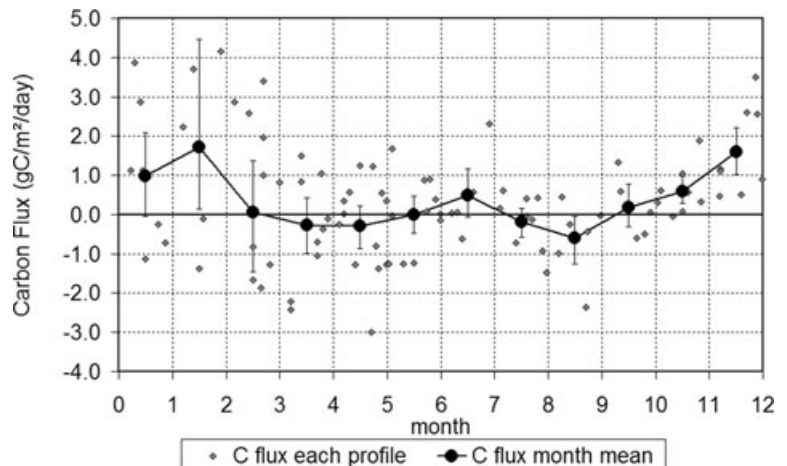

Fig. 6. CO$_2$ fluxes for each profile from 2000 to 2009 (grey diamonds), the monthly mean aggregated across all years (black circles) and the bars correspond to 95% and 5% confidence interval using a bootstrap analysis. Uncertainties for individual fluxes are not shown for clarity, but average 0.7 gC m^{-2} d^{-1}.

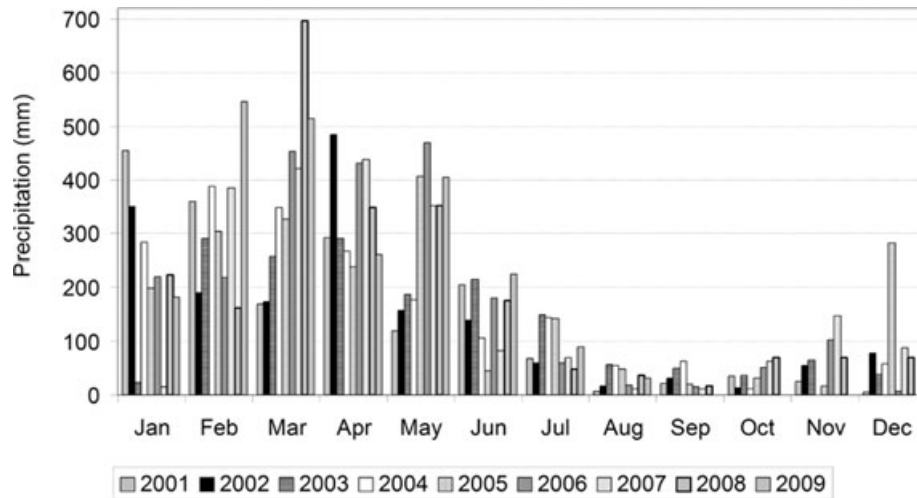*Fig. 7.* Precipitation by month for each year from http://hydis8.eng.uci.edu/hydis-unesco/ using four squares: (a) latitude from 2° to −4° and longitude from −55° to −32°; (b) latitude from −4° to −6° and longitude from −50° to −32°; (c) latitude from −6° to −8° and longitude from −45° to −32° and (d) latitude from −8° to −10° and longitude from −40° to −32°.
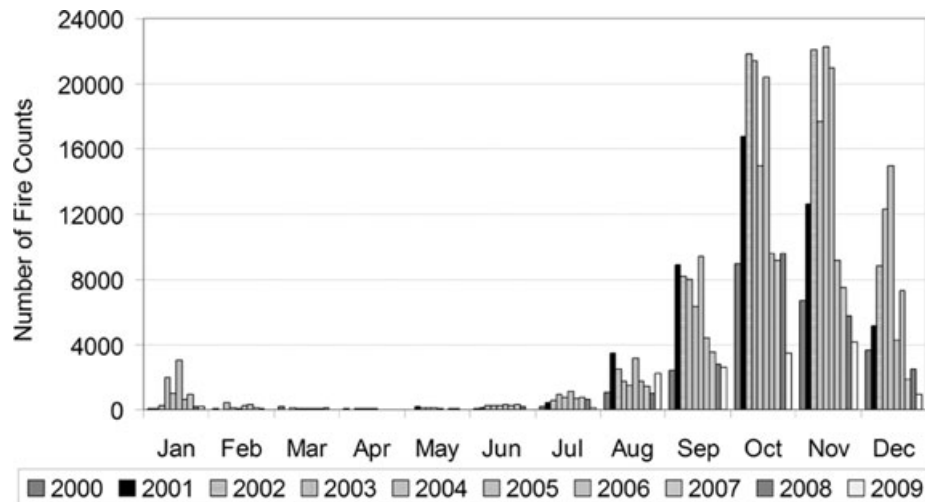

Fig. 8. Fire counts obtained from MODIS Terra/Rapid Response—NASA GSFC for the study area described in Fig. 1 (http://www.dpi.inpe.br/proarco/bdqueimadas/).

The first interesting observation given these results is the variability of flux estimates for different profiles from the same month and how this changes seasonally. The line in Fig. 6 shows clearly that this variability is generally higher during the wet season than the dry season. More specifically from January to March the variability is very high with a maximum in March. In January there is large variability, because during some years the rainy season has not started yet and thus there are still contributions from biomass burning. Although there is still high variability in February, no profiles show statistically significant sinks. During March, flux variability is the highest with some profiles showing positive and others negative fluxes. Flux variability tends to decrease throughout the rest of the year, with dry season variability clearly being lower overall than wet sea-

son. There are several significant implications of this finding. First, in order to obtain a statistically significant flux estimate during the wet season, and especially January to March, more profiles are necessary compared to the rest of the year. Second, the seasonality in variability suggests a fundamentally different impact of weather on regional scale carbon fluxes in the wet and dry seasons in eastern Amazonia. This finding parallels a model-based analysis (Parazoo et al., 2008), which showed the same behaviour but did not offer a specific explanation.

In order to understand what causes the large flux variability during the three-month period from January to March, we have investigated the relationship between precipitation a few days before the measurements and the observed fluxes. We found a maximum correlation (r^2) of 0.28 between cumulative

precipitation 3 d before the profile is measured and the flux. Inside the same wet season month a different behaviour can be found depending upon the precipitation history in the days before the flight. The correlation between precipitation and net positive flux could reflect the control of either (or both) radiation or moisture availability on NEE and its variability. Huete et al. (2006) concluded that at seasonal time scales sunlight may exert more influence than rainfall on rainforest phenology and productivity. It is not obvious that this can be generalized to day-to-day variability, however.

Finally, although we have worried about a fair weather sampling bias resulting from the requirement that light aircraft flights avoid rainy days, the fact that precipitation 3 d previous to the flight shows the maximum correlation with flux suggests the conditions on the day of the sampling are less important than the days preceding it. Although this does not eliminate the possibility of fair weather bias, for example, we have no examples of what fluxes are at day 10 of a period of 14 consecutive rainy days during the wet season, it does offer some re-assurance that this bias is not extreme. Additionally, because we see such high variability during the wet season, including both positive and negative fluxes, this also argues against a strong fair weather bias.

3.3. Using observed CO to remove fire fluxes

Another interesting observation is that the net carbon flux to the atmosphere during the wet season averages twice the flux during the dry season, when biomass is burned. To remove the influence of biomass burning on our analysis and thus identify the flux associated with NEE, we use observed CO enhancements and several $CO:CO_2$ emission ratios for biomass burning (e.g. Chou et al., 2002). This isolation of the regional NEE component of our fluxes is needed to compare our estimates to those from biometry and eddy-covariance studies, which are specifically designed to avoid the influences of biomass burning fluxes.

We use $CO:CO_2$ ratios based on our own observations. To estimate $CO:CO_2$ from our data we selected only those dry season profiles for which the biomass burning plume was very clearly identifiable in the profile. We found 20 profiles that met these rough criteria. We also avoided using the lower parts of the profile to avoid the bias originating from the influence of NEE on the observed CO_2 mole fractions (Fig. 9). The mean $CO:CO_2$ we found is 74 ± 20 ppb CO (ppm CO_2)$^{-1}$.

For comparison Andreae and Merlet (2001) published an emission ratio for tropical forests of 103 ± 14 ppb CO (ppm CO_2)$^{-1}$. While this estimate is within the uncertainty bounds of our estimate there may be reasons why the central values are different. One possibility is that as mentioned earlier, the upwind area includes not just tropical forest but also degraded forest, pasture, agricultural lands, shrub lands and savanna. The $CO:CO_2$ emission ratios for these landscapes are all less than for moist tropical forest, with savannah burning emission ratios being 63 ppb CO (ppm CO_2)$^{-1}$. Additionally, oxidation of CO by OH is also of the correct sign to explain the discrepancy, because
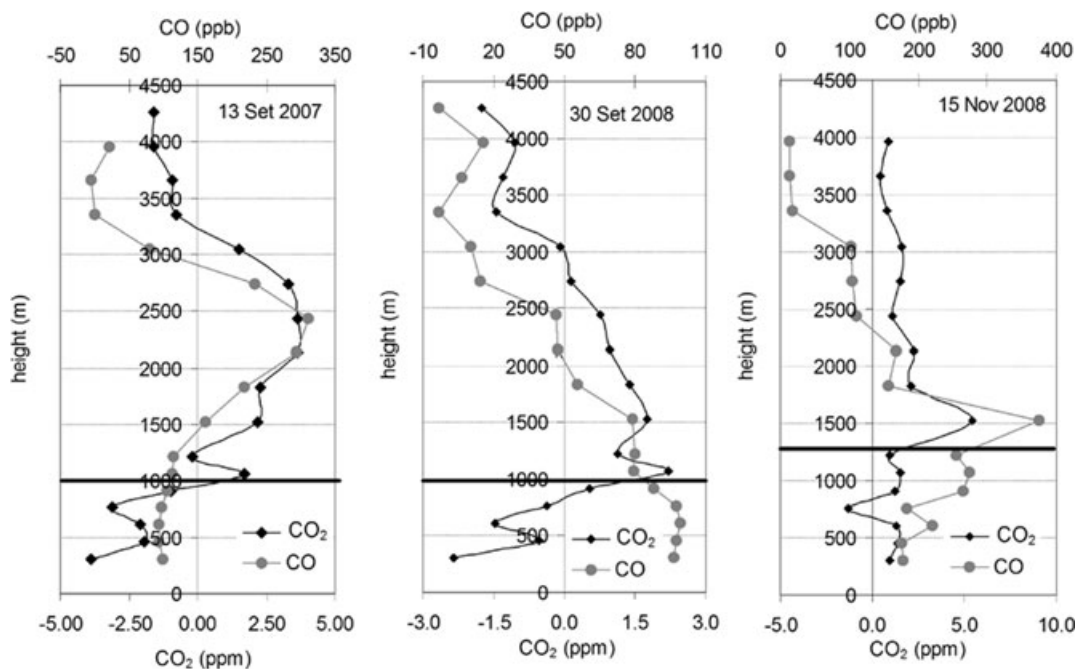

Fig. 9. CO_2 and CO vertical profiles for three different days: 09/13/2007; 09/30/2008 and 11/15/2008 illustrating the kinds of profiles used to calculate $CO:CO_2$ emission ratios from observations. The line marked the lower limit of the profile part that was used for calculating the $CO:CO_2$ ratio.

CO produced in fires will decay, while the CO_2 will not. During the tropical dry season, the OH concentration may be as high as 2.8×10^6 molecules cm^{-3} (Spivakovsky et al., 2000) implying a CO lifetime of about 20 d (Demore et al., 1997). Assuming a 2-d transit time from the combustion region implies a reduction of the true emission ratio of 10%. An additional reason for the discrepancy is suggested by Guyon et al. (2005). The smouldering fires which produce high CO:CO_2 ratios may not be hot enough to be lofted by pyro-convection into the free troposphere, where they would be more easily transported. They found a median 'detrained' ratio of 64 ppb CO (ppm CO_2)$^{-1}$. If we were trying to use our observations to determine an Amazon-wide CO:CO_2 emission ratio, this would result in a bias, but we are only trying to correct our data for the influence of burning signals, so the ratios we calculate are appropriate. Additionally, using an emission ratio of 100 instead of 74 ppb CO (ppm CO_2)$^{-1}$ has only a small impact on our results, reducing the dry season sink, but not appreciably changing the seasonality.

To correctly remove the biomass burning flux from the total net CO_2 flux we need also to take into account that there can be a natural flux of CO from soils (Conrad and Seiler, 1985) and as a by product of isoprene emissions from trees (Kuhn et al., 2007). In order to estimate the biogenic CO flux we use the observation that from March to July CO fluxes calculated of 27 mgCO m^{-2} d^{-1}, using eqs 1–3 are approximately constant (Fig. 10), although it is likely that dry season biogenic CO emissions are higher than wet season ones due to increased isoprene emissions and increased OH (Spivakovsky et al., 2000). However, for simplicity here, we assume that the stable period of biogenic CO emissions persists throughout the year, allowing us to calculate the NEE component of the total CO_2 flux as

$$F_{CO_2}^{NEE} = F_{CO_2} - r_{CO_2:CO}^{bb} \left(F_{CO} - F_{CO}^{bio} \right). \qquad (4)$$

The annual mean NEE flux is 0.02 ± 0.27 gC m^{-2} d^{-1} reduced from the total value of 0.40 gC m^{-2} d^{-1}. The monthly
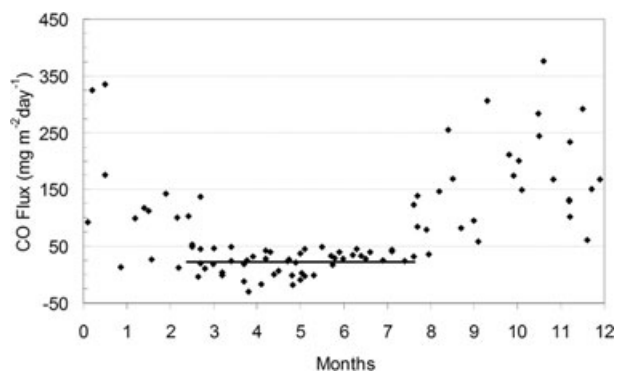
Fig. 10. CO fluxes for all profiles between 2000 and 2009. The line shows the average for the wet season time which we take to be representative of biogenic emissions throughout the year.

patterns of the total, NEE and biomass burning (bb) components are shown in Fig. 11a. After eliminating the influence of biomass burning on our analysis, the land surface is a net carbon source of 0.32 ± 0.28 gC m^{-2} d^{-1} during the wet season, and a sink of −0.24 ± 0.17 gC m^{-2} d^{-1} during the dry season. The strongest sink period is between August and November of −0.70 ± 0.21 gC m^{-2} d^{-1}. As mentioned earlier, this flux result is the sum of all non-combustion surface fluxes in the region of influence including NEE, river evasion, agricultural fluxes and any other unidentified carbon flux processes. The power of our regional scale top down approach is that we are able to estimate the sum of all fluxes, but we are unable to attribute our signal to specific processes or clearly link variability to specific mechanisms. Our study computes a carbon balance using atmospheric data, and the result is a net balance that does not try to distinguish between decomposition of organic matter in one process or another (e.g. disturbed or undisturbed ecosystem fluxes or fire). The analysis of the CO part accounts for carbon inputs from burning of forests and also agricultural burning.

Figure 11(b) shows the regional scale biological flux for eastern Amazonia from this study, with the eddy flux data from Tapajos National forest near Santarem (Saleska et al., 2003; Hutyra et al., 2007). Despite the enormous spatial scale difference represented by the two flux time series (perhaps 1 km^2 versus 100 000 km^2) they show similar seasonal variations. This result suggests that the dry season sink phenomenon is not just local but is representative of eastern Amazonia and possibly for much of Amazonia as a whole, as suggested satellite-derived Enhanced Vegetation Index too (Huete et al., 2006). The main difference between the local-scale eddy flux data and our regional scale results is the high wet season efflux, which may be due to enhanced decomposition at the Tapajos site. This was discussed by Pyle et al. (2008) and was attributed to disturbance in the mid-1990s.

Our results show clearly that the carbon uptake in eastern Amazonia occurs during the dry season, between August and November (Fig. 11a). Dry season uptake is evidenced by CO_2 depletion in the boundary layer, even when there is excess CO from fires (Fig. 9). The eddy-flux, EVI and aircraft CO_2 observations all support the hypothesis that the seasonal pattern in NEE of dry season sinks and wet season sources may be a basin-wide phenomenon, at least east of Santarem, despite substantial differences in plant communities, soils and climate across ecosystems. Our results further suggest that this and other carbon flux hypotheses could be robustly tested via a network of tower and airborne CO_2 mole fraction observations distributed across the basin. Pyle et al. (2008) and Saleska et al. (2003) both interpret the seasonal cycle in the eddy flux as due to the higher influx of solar radiation during the dry season combined with a muted or absent water limitation, our results support the view that these are large-scale mechanisms in Amazonia.
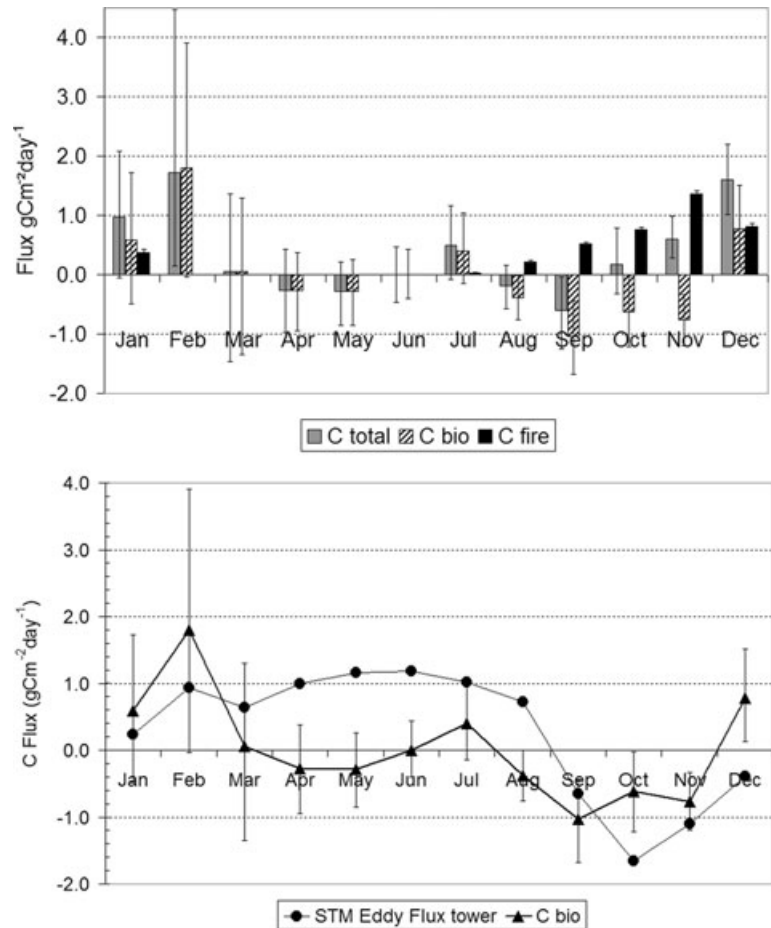
Fig. 11. (a) Monthly mean total carbon flux (grey), biological carbon flux (NEE) (striped) and carbon flux released during biomass burning (black) from 2000 to 2009. (b) Biosphere flux derived from our data for CO_2 and CO by subtracting the CO_2 inferred from biomass fires. Error bars are 90% confidence intervals from a complete bootstrap analysis including variance of the CO_2:CO ratio and CO_2 and CO concentrations. The green curve shows the monthly mean CO_2 flux at FLONA Tapajos, near Santarem, from 6 yr of eddy flux data (Pyle et al., 2008).

3.4. Uncertainty analyses

In order to address errors in our flux estimation beyond the formal propagation of uncertainty in eqs 1–3, we perform several sensitivity tests.

3.4.1. Spatial representativeness. One major question is whether our air samples are representative of large areas, or just the area near the sampling sites. Previous analyses for CH_4 (Miller et al., 2007) and N_2O (D'Amelio et al., 2009) showed samples to be representative of a large region. We repeat those same tests for CO_2 here. To assess representativeness, we compare our two profiles at SAN taken 30 km apart, and find the difference at 300 m asl ($\sim$150 m agl) to be 0.8 ± 3.5 ppm and 0.8 ± 1.5 ppm at 1200 m but only 0.4 ± 1.5 ppm at 1800 and 0.3 ± 1.6 ppm 3600 m (1σ *SD*). We further quantify this possible local impact by (1) comparing the flux calculated using the inland profiles and the river profiles and (2) re-calculating flux while eliminating the lowest measurements at 300 and 600 m, and assuming a linear vertical profile between 900 m and the surface.

The difference between fluxes calculated from measurements made above the km 67 tower and those 30 km to the east (above

a pasture landscape) (east) for 34 profiles was only 0.12 ± 0.69 gC m^{-2} d^{-1}. Then, we re-calculate flux removing the lowest points in the profile. The annual mean flux for the total profile was 0.48 ± 0.96 gC m^{-2} d^{-1}; removing the lowest point of the profile (i.e. considering heights >600 m) the flux was 0.36 ± 0.82 gC m^{-2} d^{-1} and removing the three lowest points in the profile (>1000 m) the C flux was 0.65 ± 1.03 gC m^{-2} d^{-1}. Together, these tests show only a small degree of sensitivity to local-scale (<100 km) fluxes.

3.4.2. Leakage of surface flux above 4 km. To estimate the magnitude of 'leakage' out of the top of our flux box we compare the difference between X_{bkg} and the mean mole fraction above 3 km asl, for all 85 vertical profiles. If CO_2 loss by convection is negligible, then the values above 3 km should be equal to the background value. The annual mean difference between the above 3 km value at SAN and the background value is 0.07 ± 0.87 ppm, which is negligible, compared to the variation in the air column (Fig. 5). While this is true for the annual mean, there is seasonal variation in the difference (Fig. 12a). Differences average +0.45 ± 0.84 ppm during the wet season and −0.32 ± 0.79 ppm during the dry season (Fig. 12b). If we assume that these biases persist between the top of our profiles at 4 km up
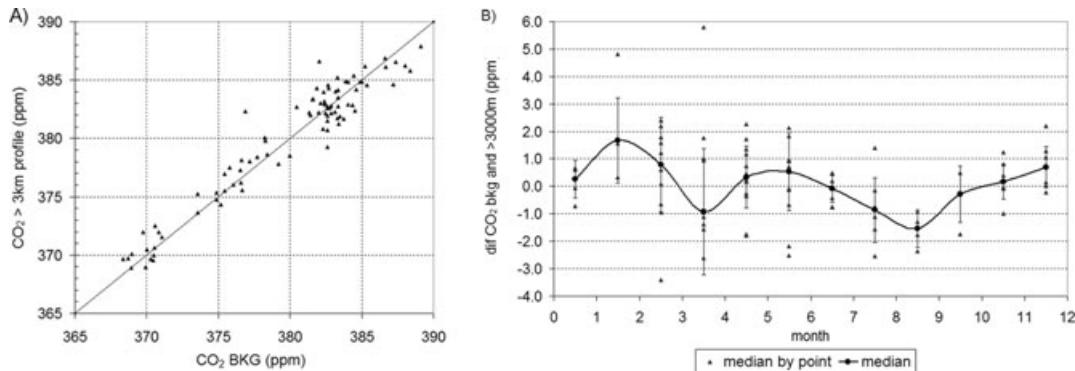
Fig. 12. (a) Linear correlation between our CO_2 calculated BKG and mean higher than 3 km. (b) The difference between background and mean >3 km for all flights and the median for each month.

to15 km asl (approximately the height of tropical tropopause), this implies wet and dry season biases in our estimated fluxes of up to 0.4 ± 0.8 and -0.3 ± 0.7 gC m^{-2} d^{-1}, respectively. The overall effect of correcting for this bias would be to increase the observed seasonal amplitude by strengthening the observed wet season source and the dry season sink. However, we caution that (a) the calculated free troposphere, background differences could also reflect seasonally varying errors in our background algorithm, which are certainly possible given the large relative seasonal cycle amplitudes present at RPB and ASC (Fig. 4) and (b) the overall correlation between the free troposphere and background is generally very good (Fig. 12a) and that the wet and dry season mean differences are perhaps best characterized by their variance and not their means.

4. Summary and conclusions

Our analysis of CO_2 vertical profile measurements made in eastern Amazonia spanning more than 9 yr reveals a regional carbon balance that shows a moderate source before correction for biomass burning fluxes. After correction for biomass burning fluxes, we calculate a nearly neutral net flux for eastern Amazonia. Despite uncertainties, our calculations rule out either large sources or sinks. Furthermore, after the minimization of biomass burning influences on our observations, a strong seasonality with an early wet season source and dry season sink emerges, very similar to that observed at the local scale by eddy covariance and biometry studies. Another prominent aspect of our results is the large difference between wet and dry season flux variability. During much of the wet season, surface source and sink behaviour is observed with nearly equal frequency, with the highest variability found in February and March. The reasons for this should be a topic of further research, although we found that precipitation explains about 30% of this variability. The high intraseasonal and interannual variability observed in fluxes also points to the necessity of conducting long-term observations in

order to understand the Amazonian carbon cycle and its sensitivity to climate. Also unknown is the extent to which our flux results can be extended beyond the region upwind (to the east) of Santarem. Because we currently have no additional aircraft sites further to the west in the Amazon basin, we can unfortunately not extend our approach to the whole basin.

We still do not know whether the Amazon basin as a whole is a carbon sink or source. However, at least for the eastern portion represented by this study the evidence suggests a moderate source when including fires and neither a source nor sink after taking account of fires. Despite the implication by Stephens et al. (2007) that after accounting for carbon release resulting from land-use change, there is a significant carbon sink in the tropics, we do not find evidence for such a sink in eastern Amazonia. This of course does not rule out sinks in other parts of Amazonia and other parts of the tropics. To detect the presence of these sinks, measurement approaches similar to the one described in this study could be deployed throughout the tropics. Based on the knowledge acquired in this study, in December 2009 we started profile measurements at three additional places further downwind in the Amazon.

5. Acknowledgments

References

Andreae, M. O. and Merlet, P. 2001. Emission of trace gases and aerosols from biomass burning. *Global Biogeochem. Cycles* **15**, 955–966.

Chou, W. W., Wofsy, S. C., Harriss, R. C., Lin, J. C., Gerbig, C. and co-authors. 2002. Net fluxes of Co2 in Amazonia derived from aircraft observations. *J. Geophys. Res.* **107**(D22), 4614, doi:10.1029/2001JD001295.

Conrad, R. and Seiler, W. 1985. Influence of temperature, moisture, and organic carbon on the flux of H2 and CO between soil and atmosphere: field studies in subtropical regions. *J. Geophys. Res.* **90**(D3), 5699–5709, doi:10.1029/JD090iD03p05699.

Conway, T. J., Tans, P. P., Waterman, L. S., Thoning, K. W., Kitzis, D. R. and co-authors. 1994. Evidence for interannual variability of the carbon cycle for the national oceanic and atmospheric administration/climate monitoring diagnostics laboratory global air sampling network. *J. Geophys. Res.* **99**, 22 831–822 855.

Cox, P. M., Betts, R. A., Jones, C. D., Spall, S. A. and Totterdell, I. J. 2000. Acceleration of global warming due to carbon-cycle feedbacks in a coupled climate model. *Nature* **408**, 184–187.

D'Amelio, M. T. S., Gatti, L. V., Miller, J. B. and Tans, P. 2009. Regional N_2O fluxes in Amazonia derived from aircraft vertical profiles. *Atmos. Chem. Phys.* **9**, 8785–8797.

Defries, R. S., Houghton, R. A., Hansen, M. C., Field, C. B., Skole, D. and co-authors. 2002. Carbon emissions from tropical deforestation and regrowth based on satellite observations for the 1980s and 1990s. *PNAS* **99**, 14 256–14 261.

Demore, W. B., Sander, S. P., Golden, D. M., Hampson, R. F., Kurylo, M. J. and co-authors. 1997. *Chemical Kinetics and Photochemical Data for Use in Stratospheric Modeling*. Jet Propulsion Laboratory, CA, USA, 266.

Draxler, R. R. and Rolph, G. D. 2003. *Hysplit (Hybrid Single-Particle Lagrangian Integrated Trajectory)*. NOAA Air Resources Laboratory, Silver Spring, MD.

Friedlingstein, P., Bopp, L., Ciais, P., Dufresne, J. L., Fairhead, L. and co-authors. 2001. Positive feedback between future climate change and the carbon cycle. *Geophys. Res. Lett.* **28**, 1543–1546.

Friedlingstein, P., Cox, P., Betts, R., Bopp, L., Von Bloh, W. and co-authors. 2006. Climate-Carbon Cycle Feedback Analysis: Results from the (Cmip)-M-4 Model Intercomparison. *J. Clim.* **19**, 3337–3353.

Gloor, M., Dlugokencky, E., Brenninkmeijer, C., Horowitz, L., Hurst, D. F. and co-authors. 2007. Three-dimensional Sf6 data and tropospheric transport simulations: signals, modeling accuracy, and implications for inverse modeling. *J. Geophys. Res.* **112**, D15112, doi:10.1029/2006JD007973.

Goulden, M. L., Munger, J. W., Fan, S. M., Daube, B. C. and Wofsy, S. C. 1996. Measurements of carbon sequestration by long-term eddy covariance: methods and a critical evaluation of accuracy. *Glob. Chan. Biol.* **2**, 169–182.

Gurney, K. R., Law, R. M., Denning, A. S., Rayner, P. J., Baker, D. and co-authors. 2002. Towards robust regional estimates of CO_2 sources and sinks using atmospheric transport models. *Nature* **415**, 626–630.

Guyon, P., Frank, G. P., Welling, M., Chand, D., Artaxo, P. and co-authors. 2005. Airborne measurements of trace gas and aerosol particle emissions from biomass burning in Amazonia. *Atmos. Chem. Phys.* **5**, 2989–3002.

Houghton, R. A. 2003. Revised estimates of the annual net flux of carbon to the atmosphere from changes in land use and land management 1850–2000. *Tellus, Ser. B* **55**, 378–390.

Huete, A. R., Didan, K., Shimabukuro, Y. E., Ratana, P., Saleska, S. R. and co-authors. 2006. Amazon rainforests green-up with sunlight in dry season. *Geophys. Res. Lett.* **33**, L06405, doi:10.1029/2005GL025583.

Hutyra, L., Munger, J. W., Saleska, S. R., Gottlieb, E. W., Daube, B. C. and co-authors. 2007. Seasonal controls on exchange of carbon and water in an Amazonian rainforest. *J. Geophys. Res. – Biogeosciences* **112**(G3), Art. No. G03008.

Jacobson, A. R., Fletcher, S. E. M., Gruber, N., Sarmiento, J. L. and Gloor, M. 2007. A joint atmosphere-ocean inversion for surface fluxes of carbon dioxide: 2, regional results. *Global Biogeochem. Cycles* **21**, GB1020, doi:10.1029/2006GB002703.

Kuhn, U., Andreae, M. O., Ammann, C., Araujo, A. C., Brancaleoni, E. and co-authors. 2007. Isoprene and monoterpene fluxes from central Amazonian rainforest inferred from tower-based and airborne measurements, and implications on the atmospheric chemistry and the local carbon budget. *Atmos. Chem. Phys.* **7**, 2855–2879.

Lapola, D. M., Oyama, M. D. and Nobre, C. A. 2009. Exploring the range of climate biome projections for tropical South America: the role of CO_2 fertilization and seasonality. *Global Biogeochem. Cycles* **23**, doi:10.1029/2008GB003357.

Lloyd, J., Kolle, O., Fritsch, H., De Freitas, S. R., Dias, M. and co-authors. 2007. An airborne regional carbon balance for central Amazonia. *Biogeosciences* **4**, 759–768.

Maiss, M., Steele, L. P., Francey, R. J., Fraser, P. J., Langenfelds, R. L. and co-authors. 1996. Sulfur hexafluoride: a powerful new atmospheric tracer. *Atmos. Environ.* **30**, 1621–1629.

Malhi, Y., Nobre, A. D., Grace, J., Kruijt, B., Pereira, M. G. P. and co-authors. 1998. Carbon dioxide transfer over a central Amazonian rain forest. *J. Geophys. Res.* **103**, 31 593–31 612.

Malhi, Y. and Phillips, O. L. 2005. *Tropical Forests and Global Atmospheric Change*. Oxford University Press, Oxford, 356pp.

Miller, J. B., Gatti, L. V., D'amelio, M. T. S., Crotwell, A., Dlugokencky, E. and co-authors. 2007. Airborne measurements indicate large methane emissions from the eastern Amazon basin. *Geophys. Res. Lett.* **34**, L10809, doi:10.1029/2006GL029213.

Olivier, J. G. J., Bouwman, A. F., Berdowski, J. J. M., Veldt, C., Bloos, J. P. J. and co-authors. 1999. Sectoral emission inventories of greenhouse gases for 1990 on per country basis as well as on 10 × 10. *Environ. Sci. Policy* **2**, 241–264.

Ometto, J., Nobre, A. D., Rocha, H. R., Artaxo, P. and Martinelli, L. A. 2005. Amazonia and the modern carbon cycle: lessons learned. *Oecologia* **143**, 483–500.

Parazoo, N. C., Denning, A. S., Kawa, S. R., Corbin, K. D., Lokupitiya, R. S. and co-authors. 2008. Mechanisms for synoptic variations of atmospheric CO_2 in north America, south America and Europe. *Atmospheric Chemistry and Physics* **8**, 7239–7254.

Phillips, O. L., Malhi, Y., Higuchi, N., Laurance, W. F., Nunez, P. V. and co-authors. 1998. Changes in the carbon balance of tropical forests: evidence from long-term plots. *Science* **282**, 439–442.

Pyle, E. H., Santoni, G. W., Nascimento, H. E. M., Hutyra, L. R., Carmago, P. B. and co-authors. 2008. Effects of disturbance on biomass, structure and carbon balance in two Amazonian Forests. *Global Biogeochem. Cycles* **113**, G00B08, doi:10.1029/2007JG000592.

Richey, J. E., Melack, J. M., Aufdenkampe, A. K., Ballester, V. M. and Hess, L. L. 2002. Outgassing from Amazonian Rivers and Wetlands as a large tropical source of atmospheric CO_2. *Nature* **416**, 617–620.

Saleska, S. R., Miller, S. D., Matross, D. M., Goulden, M. L., Wofsy, S. C. and co-authors. 2003. Carbon in Amazon forests: unexpected seasonal fluxes and disturbance-induced losses. *Science* **302**, 1554–1557.

Spivakovsky, C. M., Logan, J. A., Montzka, S. A., Balkanski, Y. J., Foreman-Fowler, M. and co-authors. 2000. Three-dimensional climatological distribution of tropospheric Oh: update and evaluation. *J. Geophys. Res.* **105**, 8931–8980.

Stephens, B. B., Gurney, K. R., Tans, P. P., Sweeney, C., Peters, W. and co-authors. 2007. Weak northern and strong tropical land carbon uptake from vertical profiles of atmospheric CO_2. *Science* **316**, 1732–1735.

Tans, P. P., Bakwin, P. S. and Guenther, D. W. 1996. A feasible global carbon cycle observing system: a plan to decipher today's carbon cycle based on observations. *Glob. Chang. Biol.* **2**, 309–318.

Thoning, K. W., Tans, P. P. and Komhyr, W. D. 1989. Atmospheric carbon dioxide at Mauna Loa observatory 2: analysis of the Noaa Gmcc Data, 1974–1985. *J. Geophys. Res.* **94**, 8549–8565.

Van Der Werf, G. R., Randerson, J. T., Collatz, G. J., Giglio, L., Kasibhatla, P. S. and co-authors. 2004. Continental-scale partitioning of fire emissions during the 1997 to 2001 El Niño/La Niña period. *Science* **303**, 73–76.

VIM3. 2007. *International Vocabulary of Metrology: Basic and General Concepts and Associated Terms. ISO/IEC Guide 99, 2007*. ISO, Geneva.

Wofsy, S. C., Harriss, R. C. and Kaplan, W. A. 1988. Carbon-dioxide in the atmosphere over the Amazon basin. *J. Geophys. Res.* **93**, 1377–1387.